SOLID MATTER

P.O. SUKHACHOV

Faculty of Physics, Taras Shevchenko National University of Kyiv
(4-g, Academician Glushkov Prosp., Kyiv 03680, Ukraine; e-mail: pavel.sukhachov@gmail.com)

PACS 71.30.+h, 71.45.Lr

GAP GENERATION IN WEYL SEMIMETALS IN A MODEL WITH LOCAL FOUR-FERMION INTERACTION

We study the gap generation in Weyl semimetals in a model with local four-fermion interaction. It is shown that there exists a critical value of coupling constant separating the symmetric and broken symmetry phases, and the corresponding phase diagram is described. The gap generation in a more general class of Weyl materials with small bare gap is studied, and the quasiparticle energy spectrum is determined. It is found that, in this case, the dynamically generated gap leads to the additional splitting of the quasiparticle energy bands.

K e y w o r d s: Weyl semimetals, gap generation, quasiparticle energy spectrum.

1. Introduction

The discovery of new materials with unique quantum-mechanical properties is crucial for the progress in condensed matter physics. Recently, such new materials as topological insulators, Dirac semimetals, and Weyl semimetals attracted the attention of the condensed matter community and moved at the forefront of theoretical and experimental studies [1–3]. Remarkable properties of these two-dimensional (2D) and 3D materials are connected with the unusual properties of their low energy quasiparticle excitations, which are described by the Dirac or Weyl equation. Since 3D massless Dirac fermions can be represented as two copies of Weyl fermions of opposite chirality, Weyl fermions can be considered as the most elementary building blocks of these 3D materials. It is important to note that while two Weyl nodes for every particle (except neutrinos, which are perhaps only left-handed fermions) in the elementary particle physics are located at $\mathbf{k} = 0$ forming thus a Dirac fermion, Weyl nodes in condensed matter physics are, in general, located at different points in the momentum space.

As is well known, graphene is a 2D Dirac semimetal. Consequently, 3D Dirac semimetals may be considered as 3D analogs of graphene. The first historically known 3D Dirac material is bismuth [4–7], whose electron states near the L point in the Brillouin zone are described by the 3D Dirac massive equation with sufficiently large Dirac mass. It is possible to decrease the Dirac mass by doping Bi with antimony. As the antimony concentration reaches $x \approx 0.03$, alloy $Bi_{1-x}Sb_x$ transforms into a Dirac semimetal with massless Dirac point, realizing thus a 3D analog of graphene. Using the *ab initio* calculations and the effective model analysis, it was further theoretically suggested in Refs. [8, 9] that Na_3Bi, K_3Bi, Rb_3Bi, and Cd_3As_2 are 3D Dirac semimetals. By investigating the electronic structure with angle resolved photoemission spectroscopy, 3D Dirac fermions were experimentally discovered in Na_3Bi in Ref. [10] and Cd_3As_2 in Refs. [11, 12]. As to the Weyl semimetals, the recent observation of negative magnetoresistivity in $Bi_{0.97}Sb_{0.03}$ provided an experimental evidence for the existence of Weyl fermions Ref. [13]. To obtain a Weyl semimetal from a Dirac semimetal, one must break either the time reversal or inversion symmetry. This can be done, for example, by applying an external magnetic field. As a result, the 3D Dirac

point splits into two Weyl nodes of opposite chiralities. A good example of the dynamical transformation of a Dirac semimetal into a Weyl one is given by the dynamical generation of the chiral shift parameter considered in Ref. [14].

Since the Coulomb interaction is not screened in Weyl semimetals due to the vanishing of the density of states at the Fermi surface, the electron-electron interactions in these materials are very important and may lead to the dynamical chiral symmetry breaking, which is connected with the dynamical gap generation due to the pairing of electrons and holes with different chiralities. In this paper, we consider the dynamical chiral symmetry breaking in Weyl semimetals in a model with local four-fermion interaction with regard for a small bare gap for quasiparticles. The gap generation in Weyl semimetals in the absence of a bare gap was previously studied in Refs. [15–17].

This paper is organized as follows. In Section 2, we introduce the model and set up the notation. The gap equation for the case of the zero bare gap is derived and solved. The dependence of the gap on the interaction strength and the momentum space separation between the Weyl nodes is determined in Section 3. The more general case of a nonzero bare gap is considered in Section 4. Using perturbation theory, we derived and solved gap equations. The energy spectrum was obtained and described. The results are summarized, and the conclusions are given in Section 5. For convenience, throughout this paper, we set $\hbar = 1$.

2. Model

We begin our study by considering the following low-energy Hamiltonian (see, Ref. [14]):

$$H^{(\mathrm{W})} = H_0^{(\mathrm{W})} + H_{\mathrm{int}}, \tag{1}$$

where

$$H_0^{(\mathrm{W})} = -\int d^3r \psi^\dagger(\mathbf{r}) \times$$
$$\times \begin{pmatrix} v_{\mathrm{F}}\boldsymbol{\sigma}(i\boldsymbol{\nabla} + \mathbf{b}_0) & \Delta_0 \\ \Delta_0 & v_{\mathrm{F}}\boldsymbol{\sigma}(-i\boldsymbol{\nabla} + \mathbf{b}_0) \end{pmatrix} \psi(\mathbf{r}) \tag{2}$$

is the Hamiltonian of the free theory, and Δ_0 is the bare gap parameter. This Hamiltonian describes two Weyl nodes of opposite chiralities separated by the vector $2\mathbf{b}_0$ in the momentum space. The opposite chiralities of Weyl nodes are required by the Nielsen–Ninomiya theorem [18]. Following Refs. [14, 19, 20], we call $\mathbf{b}_0$ the bare chiral shift parameter. Other notations: v_{F} is the Fermi velocity, and $\boldsymbol{\sigma} = (\sigma_x, \sigma_y, \sigma_z)$

are Pauli matrices associated with the band degrees of freedom [14, 21]. In the general case, the interaction Hamiltonian H_{int} describes the Coulomb interaction, i.e.,

$$H_{\mathrm{int}} = \frac{1}{2}\int d^3r d^3r' \, \psi^\dagger(\mathbf{r})\psi(\mathbf{r})U(\mathbf{r}-\mathbf{r}')\psi^\dagger(\mathbf{r}')\psi(\mathbf{r}'). \tag{3}$$

In order to simplify our calculations, we will use a model with a contact four-fermion interaction

$$U(\mathbf{r}) = \frac{e^2}{\kappa|\mathbf{r}|} \to g\,\delta^3(\mathbf{r}), \tag{4}$$

where g is a dimensionless coupling constant. As we will see, this model interaction should be sufficient for the general qualitative description of the gap generation in Weyl semimetals. Before proceeding further with the analysis, it is convenient to introduce the four-dimensional Dirac matrices in the chiral representation:

$$\gamma^0 = \begin{pmatrix} 0 & -I \\ -I & 0 \end{pmatrix}, \quad \boldsymbol{\gamma} = \begin{pmatrix} 0 & \boldsymbol{\sigma} \\ -\boldsymbol{\sigma} & 0 \end{pmatrix},$$
$$\gamma^5 \equiv i\gamma^0\gamma^1\gamma^2\gamma^3 = \begin{pmatrix} I & 0 \\ 0 & -I \end{pmatrix}, \tag{5}$$

where I is the two-dimensional unit matrix. Using the Eq. (4) and Eq. (5), we can rewrite the full Hamiltonian Eq. (1) as follows:

$$H^{(\mathrm{W})} = \int d^3r \psi^\dagger(\mathbf{r})\left(-iv_{\mathrm{F}}\gamma_0(\boldsymbol{\gamma}\boldsymbol{\nabla}) + \right.$$
$$+ v_{\mathrm{F}}\gamma_0\gamma_5(\boldsymbol{\gamma}\mathbf{b}_0) + \gamma_0\Delta\Big)\psi(\mathbf{r}) +$$
$$+ \frac{g}{2}\int d^3r \, \psi^\dagger(\mathbf{r})\psi(\mathbf{r})\psi^\dagger(\mathbf{r})\psi(\mathbf{r}). \tag{6}$$

3. Gap Equation in Weyl Semimetals without Bare Gap

3.1. Derivation of the gap equation

In this section, we derive the gap equation in Weyl semimetals using the Cornwall–Jackiw–Tomboulis formalism [22]. The Cornwall–Jackiw–Tomboulis effective action in the first order of perturbation theory takes the form:

$$\Gamma(G) = -i\,\mathrm{Tr}[\mathrm{Ln}\,G^{-1} + S^{-1}G - 1] +$$
$$+ \frac{g}{2}\int d^4r \left(\mathrm{tr}\big[G(r,r)G(r,r)\big] - \right.$$
$$- \mathrm{tr}\big[G(r,r)\big]\mathrm{tr}\big[G(r,r)\big]\Big), \tag{7}$$

where G is the full fermion propagator, and S is the free fermion propagator. The trace and the logarithm in the first term on the right-hand side of the above equation are taken in the functional sense. The Schwinger-Dyson equation for the fermion propagator determines extrema of the Cornwall–Jackiw–Tombolulis effective action and is given by

$$G^{-1}(r,r') = S^{-1}(r,r') + ig\delta^{(4)}(r-r')(G - \mathrm{tr}[G]), \quad (8)$$

where the trace is taken over spinor indices. The inverse free fermion propagator is given by

$$iS^{-1}(r,r') = (i\partial_t + iv_{\mathrm{F}}\gamma_0(\boldsymbol{\gamma}\cdot\boldsymbol{\nabla}) - $$
$$- v_{\mathrm{F}}\gamma_0\gamma_5(\boldsymbol{\gamma}\cdot\mathbf{b}_0))\,\delta^4(r-r'), \quad (9)$$

and the ansatz for the inverse full fermion propagator is given by

$$iG^{-1}(r,r') = (i\partial_t + iv_{\mathrm{F}}\gamma_0(\boldsymbol{\gamma}\cdot\boldsymbol{\nabla}) - v_{\mathrm{F}}\gamma_0\gamma_5(\boldsymbol{\gamma}\cdot\mathbf{b}) - $$
$$- \gamma_0\Delta e^{-2i(\mathbf{b}'\cdot\mathbf{r})\gamma_5})\delta^4(r-r'), \quad (10)$$

where $\mathbf{b}$ is a renormalized chiral shift, and $\Delta e^{-2i(\mathbf{b}'\cdot\mathbf{r})\gamma_5}$ is the general form of the gap term, which can be understood as the chiral charge density wave order parameter. This form of the chiral condensation, where fermions (electrons) and antifermions (holes) are paired in a state with total momentum $2\mathbf{b}'$, is reminiscent of the Larkin–Ovchinnikov–Fulde–Ferrell (LOFF) [23, 24] state of pairing between electrons with nonzero total momentum in the theory of superconductivity. Obviously, this phase can be eliminated by the chiral transformation

$$iG^{-1}(r,r') = e^{i(\mathbf{b}'\cdot\mathbf{r})\gamma_5}i\bar{G}^{-1}(r,r')e^{-i(\mathbf{b}'\cdot\mathbf{r}')\gamma_5}, \quad (11)$$

where

$$i\bar{G}^{-1}(r,r') = \left(i\partial_t + iv_{\mathrm{F}}\gamma_0(\boldsymbol{\gamma}\cdot\boldsymbol{\nabla}) - v_{\mathrm{F}}\gamma_0\gamma_5(\boldsymbol{\gamma}\cdot\bar{\mathbf{b}}) - \right.$$
$$\left. - \gamma_0\Delta\right)\delta^4(r-r') \quad (12)$$

is the inverse fermion propagator with conventional Dirac mass without chiral phase and $\bar{\mathbf{b}} = \mathbf{b} - \mathbf{b}'$. In the momentum space, Eq. (12) takes the form

$$i\bar{G}^{-1}(\omega,\mathbf{k}) = $$
$$= \begin{pmatrix} \omega - v_{\mathrm{F}}\boldsymbol{\sigma}\cdot(\mathbf{k}-\bar{\mathbf{b}}) & \Delta \\ \Delta & \omega + v_{\mathrm{F}}\boldsymbol{\sigma}\cdot(\mathbf{k}+\bar{\mathbf{b}}) \end{pmatrix}. \quad (13)$$

Multiplying the Schwinger–Dyson equation (8) by $e^{-i(\mathbf{b}'\cdot\mathbf{r})\gamma_5}$ from the left and $e^{i(\mathbf{b}'\cdot\mathbf{r}')\gamma_5}$ from the right, we obtain the equation

$$i\bar{G}^{-1}(\omega,\mathbf{k}) = i\bar{S}^{-1}(\omega,\mathbf{k}) - g(\bar{G} - \mathrm{tr}[\bar{G}]), \quad (14)$$

where $\bar{S}^{-1}(\omega,\mathbf{k})$ coincides with the inverse free propagator with $\mathbf{b}_0$ replaced by the relative chiral shift $\bar{\mathbf{b}}_0 = \mathbf{b}_0 - \mathbf{b}'$. Multiplying Eq. (14) by $\gamma^0\gamma^5\boldsymbol{\gamma}$ and taking trace, we obtain the following equation for the chiral shift parameter:

$$\bar{\mathbf{b}} = \bar{\mathbf{b}}_0 + \frac{g}{4v_{\mathrm{F}}}\mathrm{tr}\left[\gamma^0\gamma^5\boldsymbol{\gamma}\bar{G}\right]. \quad (15)$$

Further, multiplying Eq. (14) by γ_0 and taking trace, we find the gap equation

$$\Delta = \frac{g}{4}\mathrm{tr}\left[\gamma^0\bar{G}\right]. \quad (16)$$

Inverting Eq. (13), we obtain the full fermion propagator

$$i\bar{G}(\omega,\mathbf{k})N = \omega K_0 + v_{\mathrm{F}}\left(K_0\mathbf{k} - 2v_{\mathrm{F}}^2(\mathbf{k}\cdot\bar{\mathbf{b}})\bar{\mathbf{b}}\right)\gamma^0\boldsymbol{\gamma} + $$
$$+ v_{\mathrm{F}}\left[2v_{\mathrm{F}}^2(\mathbf{k}\cdot\bar{\mathbf{b}})\mathbf{k} - (K_0 - 2\Delta^2)\bar{\mathbf{b}}\right]\gamma^5\gamma^0\boldsymbol{\gamma} + $$
$$+ 2v_{\mathrm{F}}^2(\mathbf{k}\cdot\bar{\mathbf{b}})\omega\gamma^5 + \Delta\left(K_0 - 2v_{\mathrm{F}}^2\bar{\mathbf{b}}^2\right)\gamma^0 + $$
$$+ 2iv_{\mathrm{F}}^2\Delta([\bar{\mathbf{b}}\times\mathbf{k}]\cdot\boldsymbol{\gamma}) - 2\omega\Delta v_{\mathrm{F}}\gamma^5(\boldsymbol{\gamma}\cdot\bar{\mathbf{b}}), \quad (17)$$

where $K_0 = v_{\mathrm{F}}^2(\mathbf{k}^2 + \bar{\mathbf{b}}^2) + \Delta^2 - \omega^2$ and $N = K_0^2 - 4v_{\mathrm{F}}^2\left(\Delta^2\bar{\mathbf{b}}^2 + v_{\mathrm{F}}^2(\mathbf{k}\cdot\bar{\mathbf{b}})^2\right)$. We can integrate over the frequency on the right-hand side of Eqs. (15) and (16). These integrals have a similar structure and can be easily calculated

$$\int d\omega\frac{A_1 + A_2\omega^2}{(\omega^2 + W_1)(\omega^2 + W_2)} = $$
$$= \frac{\pi}{\sqrt{W_1} + \sqrt{W_2}}\left(A_2 + \frac{A_1}{\sqrt{W_1 W_2}}\right), \quad (18)$$

where $W_{1,2} = \left(\Delta^2 + v_{\mathrm{F}}^2(\mathbf{k}^2 + \bar{\mathbf{b}}^2)\right) \mp \sqrt{K_0^2 - N}$. Thus, we obtain the following system of equations:

$$1 = g\int\frac{d^3\mathbf{k}}{(2\pi)^4}\frac{\pi}{\sqrt{W_1} + \sqrt{W_2}} \times $$
$$\times\left(1 + \frac{v_{\mathrm{F}}^2(\mathbf{k}^2 - \bar{\mathbf{b}}^2) + \Delta^2}{\sqrt{W_1 W_2}}\right), \quad (19)$$

$$\bar{\mathbf{b}} = \bar{\mathbf{b}}_0 - g\int\frac{d^3\mathbf{k}}{(2\pi)^4}\frac{\pi}{\sqrt{W_1} + \sqrt{W_2}} \times $$
$$\times\left(\bar{\mathbf{b}} + \frac{\bar{\mathbf{b}}\left(v_{\mathrm{F}}^2(\bar{\mathbf{b}}^2 + \mathbf{k}^2) - \Delta^2\right) - 2\mathbf{k}v_{\mathrm{F}}^2(\bar{\mathbf{b}}\cdot\mathbf{k})}{\sqrt{W_1 W_2}}\right). \quad (20)$$

3.2. Solution with chiral phase

In this case, fermions and antifermions are paired with non-zero total momentum. One can easily prove that $\bar{\mathbf{b}} = 0$ if we choose $\mathbf{b}' = \mathbf{b}_0$, which leads to $\bar{\mathbf{b}}_0 = 0$. Then Eq. (19) equals

$$
\begin{aligned}
1 &= g \int \frac{d^3\mathbf{k}}{(2\pi)^4} \frac{\pi}{\sqrt{\Delta^2 + v_F^2 k^2}} = \\
&= 4g\pi^2 \int_0^\Lambda \frac{k^2 dk}{(2\pi)^4} \frac{1}{\sqrt{\Delta^2 + v_F^2 k^2}} = \\
&= \frac{g\Lambda^2}{8v_F\pi^2} \left(\sqrt{\left(\frac{\Delta}{v_F\Lambda}\right)^2 + 1} - \right. \\
&\quad \left. - \left(\frac{\Delta}{v_F\Lambda}\right)^2 \operatorname{arcsinh}\left(\frac{v_F\Lambda}{\Delta}\right) \right),
\end{aligned}
\tag{21}
$$

where $\Lambda = \frac{\pi}{a}$ is a momentum cutoff, and a is the lattice spacing. Assuming that $\frac{\Delta}{v_F\Lambda} \ll 1$, Eq. (21) simplifies to the following one:

$$
\begin{aligned}
\frac{1}{g} - \frac{1}{g_{cr}} &\approx \frac{\Delta^2}{16 v_F^3 \pi^2} \left(1 + 2\ln\left(\frac{\Delta}{2v_F\Lambda}\right) \right), \\
g_{cr} &= \frac{8\pi^2 v_F}{\Lambda^2},
\end{aligned}
\tag{22}
$$

where g_{cr} is the critical value of coupling constant.

One can see from Eq. (22) and Fig. 1 that the coupling constant g must exceed a critical value g_{cr} in order to produce a non-trivial gap Δ. Of course, there is also the trivial solution $\Delta = 0$. To determine the solution with the lowest energy, we will calculate the value of Cornwall–Jackiw–Tomboulis effective action at its extrema, which gives the energy of the system. After some calculations (for more details, see Appendix)), we find the energy density of the system

$$
\begin{aligned}
\mathcal{E} = -\frac{\Lambda^4 v_F}{8\pi^2} &\left[\sqrt{\left(\frac{\Delta}{v_F\Lambda}\right)^2 + 1} \left(2 - \left(\frac{\Delta}{v_F\Lambda}\right)^2\right) + \right. \\
&\left. + \left(\frac{\Delta}{v_F\Lambda}\right)^4 \operatorname{arcsinh}\left(\frac{v_F\Lambda}{\Delta}\right) \right].
\end{aligned}
\tag{23}
$$

Since $\mathcal{E}(\Delta \neq 0) - \mathcal{E}(\Delta = 0) < 0$ for $\frac{\Delta}{v_F\Lambda} < 1$, a non-trivial solution is always more favorable as soon as it exists. Our results coincide with those obtained in Refs. [15–17].

3.3. Phase diagram

In this subsection, we compare three different phases that can exist in the system. The solution with the chiral phase was studied in the previous subsection. In the case of the Dirac phase, fermions and antifermions are paired with zero total momentum that means $\mathbf{b}' = 0$. Thus, we have the usual Dirac mass term $\gamma_0 \Delta$ in Eq. (10), and there is no need in the chiral transformation (11). Moreover, there is the normal phase, where $\Delta = 0$. For both normal and Dirac phases, Eqs. (19) and (20) retain their forms, but with the replacement $\bar{\mathbf{b}} \to \mathbf{b}$. Without any loss of generality, we can assume that $\mathbf{b}_0$ and $\mathbf{b}$ point in the $+z$ direction. Equations (19) and (20) were solved numerically by using *Mathematica* and the iteration procedure with the following values of constants: $v_F = 3.5 \times 10^5$ m/s, $\Lambda = \frac{\pi}{a} = 2.65 \times 10^9\,\mathrm{m}^{-1}$ (according to Ref. [25], for $\mathrm{Bi}_{0.88}\mathrm{Sb}_{0.12}$, $a = 1.18\,\mathrm{nm}$). The domain of existence of the Dirac phase is plotted in Fig. 2, where the Dirac phase exists to the right from the critical line separating the symmetric normal phase and the Dirac phase with broken symmetry.

To obtain the full phase diagram, it is important to compare the energy density of the chiral (or LOFF-like) phase $\mathcal{E}(b' \neq 0, \Delta \neq 0)$, with the energy density of the normal $\mathcal{E}(\Delta = 0)$ and Dirac $\mathcal{E}(b' = 0, \Delta \neq 0)$, phases, using the expression for the energy density given by Eq. (A10) in Appendix. In this subsection, we will use $g = 1.05 g_{cr}$. Using Eqs. (A10) and (17), we calculate the energy densities of these phases as functions of b_0. The difference of the energy densities of the normal and chiral phases and the difference of
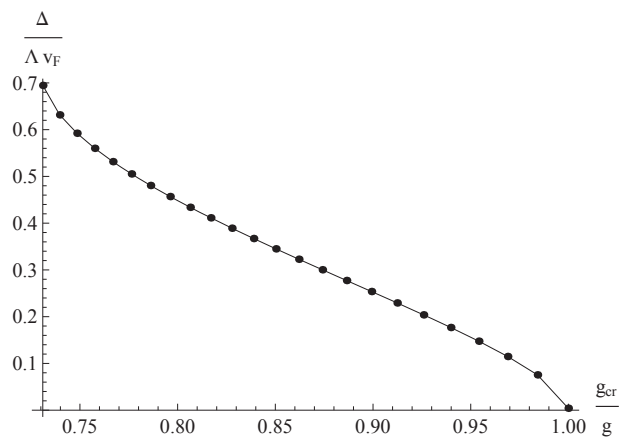

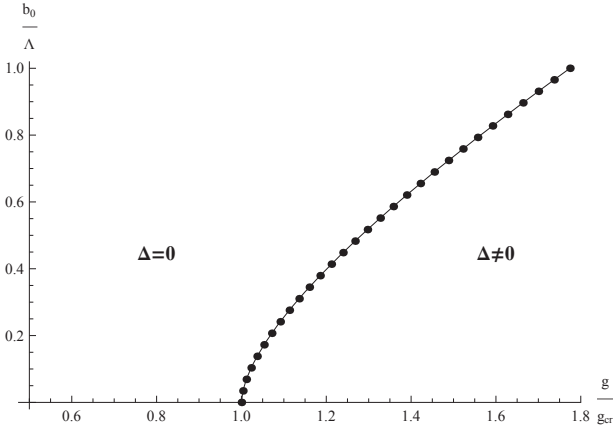
Fig. 1. Gap as a function of g_{cr}/g
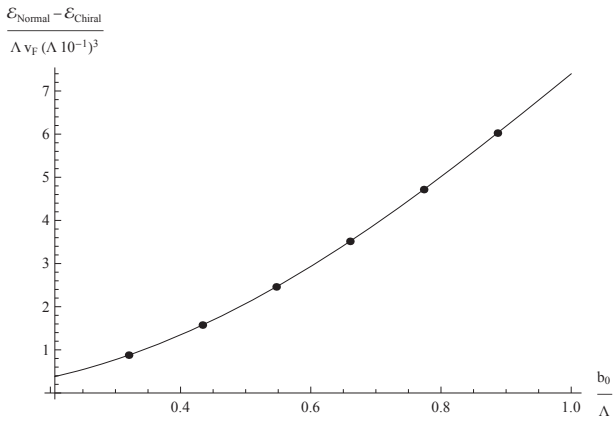
Fig. 2. Domain of existence of the Dirac phase

Fig. 4. Difference of the energy densities $\mathcal{E}_{\mathrm{Dirac}} - \mathcal{E}_{\mathrm{Chiral}}$ as a function of b_0

Fig. 3. Difference of the energy densities $\mathcal{E}_{\mathrm{Normal}} - \mathcal{E}_{\mathrm{Chiral}}$ as a function of b_0

Fig. 5. Phase diagram of the system

the energy densities of the Dirac and chiral phases are plotted in Figs. 3 and 4, respectively.

We found that the phase diagram of the system is simple. For $g > g_{\mathrm{cr}}$, the chiral phase has a lower energy compared to that of the normal and Dirac phases. The phase diagram of the system is plotted in Fig. 5.

4. Gap Equation in Weyl Semimetals with Bare Gap Δ_0

4.1. Derivation of the gap equation

Let us consider a more general case of Weyl semimetal-like materials with bare gap Δ_0. This case is of interest from the theoretical and experimental viewpoints. For example, quasiparticle excitations in $\mathrm{Bi}_{1-x}\mathrm{Sb}_x$ are described by massless Dirac fermions only at one point $x = 0.03$; otherwise, a non-ze-
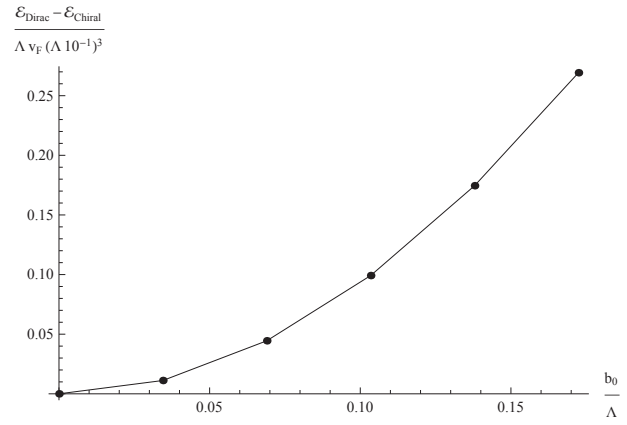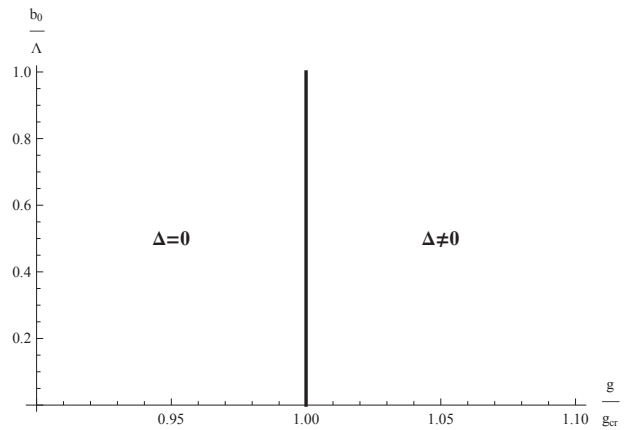
ro mass for Dirac quasiparticles is present. Using Eq. (6), it is easy to obtain the inverse free propagator

$$iS^{-1}(r, r') = (i\partial_t + iv_{\mathrm{F}}\gamma_0(\boldsymbol{\gamma} \cdot \boldsymbol{\nabla} -$$
$$- v_{\mathrm{F}}\gamma_0\gamma_5(\boldsymbol{\gamma} \cdot \mathbf{b}_0) - \gamma_0\Delta_0) \, \delta^4(r - r'). \tag{24}$$

As to the inverse full fermion propagator, the generalization of ansatz (13) to the case under consideration is given by

$$iG_1^{-1}(r, r') = (i\partial_t + iv_{\mathrm{F}}\gamma_0(\boldsymbol{\gamma} \cdot \boldsymbol{\nabla}) - v_{\mathrm{F}}\gamma_0\gamma_5(\boldsymbol{\gamma} \cdot \mathbf{b}) -$$
$$- \gamma_0(\Delta_1 + \Delta e^{-2i(\mathbf{b}' \cdot \mathbf{r})\gamma_5}))\delta^4(r - r'). \tag{25}$$

To proceed further with the Schwinger–Dyson equation (8), we must calculate the fermion propagator. However, due to Δ_0 and Δ_1 terms in the inverse full fermion propagator (25), the chiral phase

factor $e^{-2i(\mathbf{b}'\cdot\mathbf{r})\gamma_5}$ cannot be removed by the chiral transformation (11). Therefore, we cannot proceed as straightforwardly as in Section 3. Since we assume that Δ_0 is small, and Δ_1 is proportional to Δ_0, we use perturbation theory in Δ_1. We have

$$G_1(r, r') = G(r, r') + \Delta_1 F(r, r'), \qquad (26)$$

where $G(r, r')$ is the fermion propagator, which corresponds to the case $\Delta_1 = 0$. To find $F(r, r')$, we use the equation

$$\int d^4 r' G_1^{-1}(r, r') G_1(r', r'') = \delta^4(r - r''). \qquad (27)$$

In the first order in Δ_1, we find

$$\gamma_0 i G(r, r'') + \int d^4 r' G^{-1}(r, r') F(r', r'') = 0. \qquad (28)$$

It is convenient to factor out the chiral phase in the inverse full and full fermion propagators

$$\begin{aligned} G^{-1}(r, r') &= e^x \bar{G}^{-1}(r, r') e^{-x'}, \\ G(r, r') &= e^x \bar{G}(r, r') e^{-x'}, \end{aligned} \qquad (29)$$

where $\bar{G}(r, r')$ is the fermion propagator without the chiral phase, and $x \equiv i(\mathbf{b}' \cdot \mathbf{r})\gamma_5$, $x' \equiv i(\mathbf{b}' \cdot \mathbf{r}')\gamma_5$. Multiplying Eq. (28) by $-ie^{x'''}\bar{G}(r''', r)e^{-x}$ and integrating over r, we obtain

$$\int d^4 r e^{x'''} \bar{G}(r''', r) e^{-x} \gamma_0 e^x \bar{G}(r, r'') e^{-x''} = $$
$$= iF(r''', r''). \qquad (30)$$

The Schwinger–Dyson equation (8) takes the following form:

$$i\bar{G}^{-1}(r, r') - \gamma_0 \Delta_1 \delta^{(4)}(r - r') e^{2x'} = $$
$$= e^{-x} iS^{-1}(r, r') e^{x'} - g\delta^{(4)}(r - r')\Big(\bar{G}(r, r') + $$
$$+ \Delta_1 e^{-x} F(r, r') e^{x'} - e^{-x} \text{tr}[G_1] e^{x'}\Big). \qquad (31)$$

Multiplying Eq. (31) by γ_0 and taking trace, we have

$$4\Delta_1 \cos 2(\mathbf{b}' \cdot \mathbf{r}) + 4\Delta = 4\Delta_0 \cos 2(\mathbf{b}' \cdot \mathbf{r}) + $$
$$+ g\, \text{tr}[\bar{G}_0(r, r)\gamma_0] + g\Delta_1 \text{tr}[e^{-x} F(r, r) e^x \gamma_0]. \qquad (32)$$

The equation for Δ is the same as in Section 3 and can be easily written in the explicit form. Now, we can proceed with the F term:

$$\text{tr}[e^{-x} iF(r, r) e^x \gamma_0] = $$

$$= \text{tr}\Big[\int d^4 r' \bar{G}(r, r') e^{-2x'} \gamma_0 \bar{G}(r', r)\gamma_0\Big]. \qquad (33)$$

Expressing $\bar{G}(r, r')$ through its Fourier transform in the momentum space and integrating over r, we find

$$\text{tr}[e^{-x} iF(r, r) e^x \gamma_0] = \text{tr}\Big[\int \frac{d\omega_1 d^3\mathbf{k}_1}{(2\pi)^4} \frac{d\omega_2 d^3\mathbf{k}_2}{(2\pi)^4} \times $$
$$\times \bar{G}(\omega_1, \mathbf{k}_1)(2\pi)^4 \delta(\omega_1 - \omega_2)\delta(\mathbf{k}_1 - \mathbf{k}_2 - 2\mathbf{b}'\gamma_5) \times $$
$$\times e^{it'(\omega_1 - \omega_2) - i\mathbf{r}(\mathbf{k}_2 - \mathbf{k}_1)} \gamma_0 \bar{G}(\omega_2, \mathbf{k}_2)\gamma_0\Big], \qquad (34)$$

where $\delta(\mathbf{k}_1 - \mathbf{k}_2 + 2\mathbf{b}'\gamma_5)$ is a matrix 4×4 which can be written as:

$$\delta(\mathbf{k}_1 - \mathbf{k}_2 - 2\mathbf{b}'\gamma_5) = \frac{1 + \gamma_5}{2} \delta(\mathbf{k}_1 - \mathbf{k}_2 - 2\mathbf{b}') + $$
$$+ \frac{1 - \gamma_5}{2} \delta(\mathbf{k}_1 - \mathbf{k}_2 + 2\mathbf{b}'). \qquad (35)$$

Integrating over ω_1 and $\mathbf{k}_1$, Eq. (34) can be rewritten as follows:

$$\text{tr}[e^{-x} iF(r, r) e^x \gamma_0] = \text{tr}\Big[\int \frac{d\omega_2 d^3\mathbf{k}_2}{(2\pi)^4} \times $$
$$\times \big(\bar{G}(\omega_2, \mathbf{k}_2 + 2\mathbf{b}')P_+ + \bar{G}(\omega_2, \mathbf{k}_2 - 2\mathbf{b}')P_-\big) \times $$
$$\times e^{2x} \bar{G}(\omega_2, -\mathbf{k}_2)\Big], \qquad (36)$$

where $P_\pm = \frac{1 \pm \gamma_5}{2}$. Equation (36) gives contributions only with the $\cos 2(\mathbf{b}' \cdot \mathbf{r})$ and $\sin 2(\mathbf{b}' \cdot \mathbf{r})$ terms. The sine term is approximately by 8 orders smaller than the leading cosine term and will be neglected. This term is related to the approximations that were used in the derivation of the gap equation. Thus, the gap equation (32) is equivalent to the following system of equations:

$$\begin{aligned} \Delta_1 &= \Delta_0 + \frac{g}{4}\Delta_1 \text{tr}[e^{-x} F(r, r) e^x \gamma_0], \\ \Delta &= \frac{ig}{4} \text{tr}[-i\bar{G}(r, r)\gamma_0]. \end{aligned} \qquad (37)$$

To obtain the equation for the chiral shift parameter, we multiply Eq. (31) by $\gamma^0 \gamma^5 \boldsymbol{\gamma}$ and take trace

$$\bar{\mathbf{b}} = \bar{\mathbf{b}}_0 + \frac{g}{4} \text{tr}[\gamma^0 \gamma^5 \boldsymbol{\gamma} \bar{G}_0(r, r)] + $$
$$+ \frac{g\Delta_1}{4} \text{tr}[\gamma^0 \gamma^5 \boldsymbol{\gamma} e^{-x} F(r, r) e^x]. \qquad (38)$$
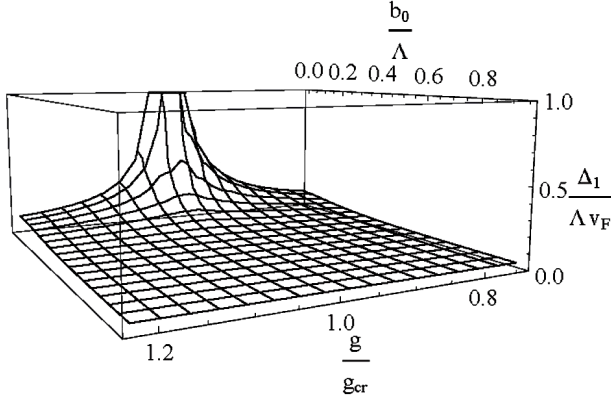
Fig. 6. Dependence of Δ_1 on the coupling constant and the chiral shift parameter

Further,

$$\mathrm{tr}[\gamma^0\gamma^5\boldsymbol{\gamma}e^{-x'}iF(r',r')e^{x'}] = \mathrm{tr}\bigg[\gamma^5\boldsymbol{\gamma}\int\frac{d\omega_2 d^3\mathbf{k}_2}{(2\pi)^4}\times$$

$$\times\left(\bar{G}(\omega_2,\mathbf{k}_2+2\mathbf{b}')P_+ + \bar{G}(\omega_2,\mathbf{k}_2-2\mathbf{b}')P_-\right)\times$$

$$\times e^{2x'}\bar{G}(\omega_2,-\mathbf{k}_2)\bigg]. \tag{39}$$

This term also can generate only the sine and cosine terms. Therefore, in order to be consistent with the initial ansatz for the fermion propagator Eq. (26), we should neglect them in the equation for the chiral shift parameter. So, we have

$$\bar{\mathbf{b}} = \bar{\mathbf{b}}_0 + \frac{g}{4}\,\mathrm{tr}[\gamma^0\gamma^5\boldsymbol{\gamma}\bar{G}(r,r)], \tag{40}$$

which is equivalent to Eq. (15). Further, using Eq. (17) and performing the Wick rotation, we can obtain the following equation for Δ_1:

$$\Delta_1 = \Delta_0 + \int\frac{d\omega_E d^3\mathbf{k}}{(2\pi)^4}g\Delta_1\times$$

$$\times\bigg(\frac{(v_F^2 k^2+\omega_E^2)^2-\Delta^4}{K_1(\omega_E,\mathbf{k})K_1(\omega_E,\mathbf{k}-2\mathbf{b}')K_1(\omega_E,\mathbf{k}+2\mathbf{b}')}-$$

$$-\frac{4b_z'^2 v_F^2\left(k^2 v_F^2\cos(2\theta)-W^2+\Delta^2\right)}{K_1(\omega_E,\mathbf{k})K_1(\omega_E,\mathbf{k}-2\mathbf{b}')K_1(\omega_E,\mathbf{k}+2\mathbf{b}')}\bigg). \tag{41}$$

where $K_1(\omega_E,\mathbf{k}) = v_F^2\mathbf{k}^2+\Delta^2+\omega_E^2$. It is worth mentioning that the equations for Δ and $\mathbf{b}$ given by Eqs. (37) and (40) coincide with Eqs. (19) and (20).

4.2. Solutions

Equation (41) is solved numerically in the case of $\mathbf{b}' = \mathbf{b}_0$ and $\mathbf{b}_0 = \{0,0,b_0\}$, by using *Mathematica*. Further, we use the following values of constants: $v_F = 3.5\times 10^5$ m/s, $\Lambda = \frac{\pi}{a} = 2.65\times 10^9$ m^{-1} (according to Ref. [25], for $\mathrm{Bi}_{0.88}\mathrm{Sb}_{0.12}$, $a = 1.18$ nm), and $\Delta_0 = 0.021$ eV (according to Ref. [25]). Numerical solutions of Eq. (41) are plotted in Fig. 6.

4.3. Quasiparticle energy spectrum

In the previous subsection, we have found Δ_1 and Δ. Let us determine the energy spectrum of the system with the dynamically generated Δ_1 and Δ. Assuming without any loss of generality that $\mathbf{b}_0$ points in the $+z$ direction and performing the chiral transformation (11), we can rewrite the Hamiltonian of the system as follows:

$$H = v_F\gamma_0(\gamma_x k_x + \gamma_y k_y) - iv_F\gamma_0\gamma_z\partial_z +$$

$$+\gamma_0\Delta + \gamma_0\Delta_1 e^{2ib_0 z\gamma_5}. \tag{42}$$

The last term is periodic and has a small amplitude, so we have a standard situation similar to the model of nearly free electron in the solid-state physics. Thus, the quasiparticle energy zone splits into additional zones near the boundaries of a new Brillouin zone. According to Ref. [26], we can write the quasiparticle energy spectrum in the first order of perturbation theory ($\Delta_1 \ll \Delta$), i.e.,

$$\epsilon_k^0 = \pm\sqrt{v_F^2\mathbf{k}_\perp^2 + v_F^2 k_z^2 + \Delta^2},$$

$$\epsilon_k^\pm = \frac{\epsilon_k^0+\epsilon_{k-K}^0}{2}\pm\frac{1}{2}\sqrt{\left(\epsilon_k^0-\epsilon_{k-K}^0\right)^2+4U_K U_{-K}}, \tag{43}$$

where $K = 2b_0$ is the inverse lattice vector of a new Brillouin zone and,

$$U_K = \frac{b_0}{\pi}\int\limits_{-\frac{\pi}{2b_0}}^{\frac{\pi}{2b_0}}dz e^{-iKz}\gamma_0\Delta_1 e^{2ib_0 z\gamma_5} =$$

$$= \frac{-4\Delta_1 b_0\gamma_0}{\pi}\sin\left(\frac{K\pi}{2b_0}\right)\times$$

$$\times\left(P_+\frac{1}{K-2b_0} + P_-\frac{1}{K+2b_0}\right) =$$

$$= -2\Delta_1\gamma_0\left(P_+\delta_{K,2b_0} + P_-\delta_{K,-2b_0}\right). \tag{44}$$
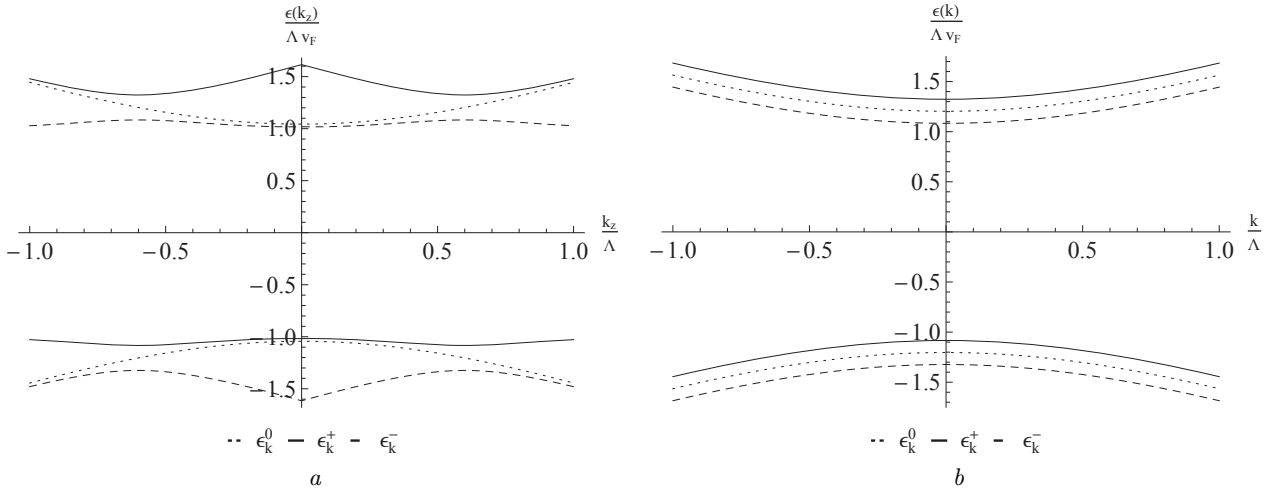
Fig. 7. Quasiparticle energy spectrum in the first order of perturbation theory for the chiral shift $b_0 = 0.6 \times \Lambda$ as a function of: (a) k_z with $k = 0$, (b) k with $k_z = b_0$. Solid lines correspond to ϵ_k^+, dashed lines to ϵ_k^-, and dotted lines to the zero order of perturbation theory

To plot the energy spectrum of quasiparticles, we can use the following numerical values: $v_{\rm F} \approx 3.5 \times 10^5$ m/s, $g = 1.2 g_{\rm cr}$, $\Delta = 0.64$ eV. For the given g, the gap in Fig. 6 is well fitted by $\Delta_1 = \frac{1+c_1 y^2+c_2 y^4}{c_3+c_4 y^2+c_5 y^4} \times (\Lambda v_{\rm F})$ with fitting parameters $c_1 = 7.8$, $c_2 = 19.1$, $c_3 = 7.4$, $c_4 = 106.8$, $c_5 = 453.2$, and $y = \frac{b_0}{\Lambda}$. We plot the energy spectrum in Fig. 7.

5. Discussion and Summary

We have studied the gap generation in Weyl semimetals, by using a model with local Coulomb interaction. We have showed that there is a critical value of coupling constant $g_{\rm cr}$, which separates the symmetric phase and the phase with broken symmetry. The phase diagram of the system is displayed in Fig. 5 in the plane of coupling constant and chiral shift parameter. Further, the gap generation in Weyl semimetals-like materials with small bare gap was studied. The non-zero bare gap considerably complicates the analysis, because the chiral phase in the ansatz for the inverse full fermion propagator cannot be removed by the chiral transformation. The solution in this case is displayed in Fig. 6. Obviously, the chiral shift parameter inhibits the gap generation, because the larger $|\mathbf{b_0}|$, the smaller the gap Δ_1. Further, the quasiparticle energy spectrum was determined, and it is found that the simultaneous presence of gaps Δ_1 and $\Delta e^{-2ib_0 z\gamma_5}$ leads to the additional splitting of the quasiparticle energy bands shown in Fig. 7.

In the present study, we have analyzed a simple model with two Weyl nodes and a contact four-fermion interaction. In real materials, such as tellurium, bismuth, and antimony heterostructures, the more realistic Coulomb interaction and the anisotropy should be taken into account. The corresponding analysis will be done and reported elsewhere. However, we believe that our qualitative results will survive in the case of more realistic models.

APPENDIX
Free energy density

In this Appendix, we will focus on the derivation of the free energy density. Since the Schwinger–Dyson equation (8) implies that

$$\frac{g}{2} \int d^4 r \left({\rm tr}[G(r,r)G(r,r)] - {\rm tr}[G(r,r)]{\rm tr}[G(r,r)] \right) =$$

$$= -\frac{i}{2} \left(1 - S^{-1}G \right), \tag{A1}$$

the energy density can be rewritten as follows:

$$\mathcal{E} = i{\rm Tr} \left({\rm Ln}G^{-1} + \frac{1}{2}(S^{-1}G - 1) \right) =$$

$$= i \int_{-\infty}^{\infty} \frac{d\omega}{2\pi} {\rm Tr} \left[{\rm Ln}G^{-1} + \frac{1}{2}(S^{-1}G - 1) \right] =$$

$$= i \int_{-\infty}^{\infty} \frac{d\omega}{2\pi} {\rm Tr} -\omega \frac{\partial G^{-1}(\omega)}{\partial \omega} G(\omega) + +\frac{1}{2}(S^{-1}(\omega)G(\omega) - 1) \Big]. \tag{A2}$$

Using the relation

$$\frac{\partial i G^{-1}(\omega; \mathbf{r}, \mathbf{r}')}{\partial \omega} = \delta(\mathbf{r} - \mathbf{r}'), \tag{A3}$$

we find

$$\mathcal{E} = i \int\limits_{-\infty}^{\infty} \frac{d\omega}{2\pi} \operatorname{tr}\left[i\omega G(\omega; \mathbf{0}) + \right.$$

$$\left. + \frac{1}{2} \int d^3 \mathbf{r} S_0^{-1}(\omega; \mathbf{r}) G(\omega; -\mathbf{r}) \right] - \mathcal{E}_0, \tag{A4}$$

where $\mathcal{E}$ is the energy density. It is convenient to perform the Fourier transformation

$$\mathcal{E} = i \int \frac{d\omega d^3 \mathbf{k}}{(2\pi)^4} \operatorname{tr}\left[i\omega G(\omega; \mathbf{k}) + \frac{1}{2} S^{-1}(\omega; \mathbf{k}) G(\omega; \mathbf{k}) \right] - \mathcal{E}_0. \tag{A5}$$

Using Eq. (17) and assuming that $\bar{b} = 0$ and $\mathbf{b}_0$ points in the $+z$ direction, we obtain

$$\mathcal{E} = 2i \int \frac{d\omega d^3 \mathbf{k}}{(2\pi)^4} \frac{v_{\mathrm{F}}^2 k^2 + \omega^2}{v_{\mathrm{F}}^2 k^2 - \omega^2 + \Delta^2} - \mathcal{E}_0 =$$

$$= -\frac{\Lambda^4 v_{\mathrm{F}}}{8\pi^2}\left[\sqrt{\left(\frac{\Delta}{v_{\mathrm{F}}\Lambda}\right)^2 + 1}\left(2 - \left(\frac{\Delta}{v_{\mathrm{F}}\Lambda}\right)^2 \right) + \right.$$

$$\left. + \left(\frac{\Delta}{v_{\mathrm{F}}\Lambda}\right)^4 \operatorname{arcsinh}\left(\frac{v_{\mathrm{F}}\Lambda}{\Delta}\right) \right] - \tilde{\mathcal{E}}_0, \tag{A6}$$

where the constant $\tilde{\mathcal{E}}_0$ can be omitted.

In the case $\bar{b} \neq 0$, there are some subtleties in the determination of the energy density of the system. Performing the chiral transformation (11), one must be careful with the integral boundaries. To account for this fact, we can represent Eq. (A5) in the terms of the left- and right-hand sides:

$$\mathcal{E} = i \int \frac{d\omega d^3 \mathbf{k}}{(2\pi)^4} \operatorname{tr}[(P_{\mathrm{L}} + P_{\mathrm{R}}) i\omega G(\omega; \mathbf{k}) +$$

$$+ (P_{\mathrm{L}} + P_{\mathrm{R}})\frac{1}{2} S^{-1}(\omega; \mathbf{k}) G(\omega; \mathbf{k})] = \mathcal{E}_{\mathrm{L}} + \mathcal{E}_{\mathrm{R}}. \tag{A7}$$

If we perform the chiral transformation (11), then we must redefine the limits of integration as follows:

$$\mathcal{E}_{\mathrm{L}}: \int\limits_{-\Lambda}^{\Lambda} dk_z \to \int\limits_{-\Lambda - b_0}^{\Lambda - b_0} dk_z, \quad \mathcal{E}_{\mathrm{R}}: \int\limits_{-\Lambda}^{\Lambda} dk_z \to \int\limits_{-\Lambda + b_0}^{\Lambda + b_0} dk_z. \tag{A8}$$

For the integral over ω, one can use Eq. (A7) and Eq. (17). We have the typical integral

$$\int \frac{d\omega_{\mathrm{E}} d^3 \mathbf{k}}{(2\pi)^4} \frac{\omega_{\mathrm{E}}^4 + \omega_{\mathrm{E}}^2 A_2 + A_1}{(\omega_{\mathrm{E}}^2 + W_1)(\omega_{\mathrm{E}}^2 + W_2)} =$$

$$= \int \frac{d\omega_{\mathrm{E}} d^3 \mathbf{k}}{(2\pi)^4}\left(1 - \frac{\omega_{\mathrm{E}}^2(A_2 - W_1 - W_2) + A_1 - W_1 W_2}{(\omega_{\mathrm{E}}^2 + W_1)(\omega_{\mathrm{E}}^2 + W_2)} \right), \tag{A9}$$

where A_1 and A_2 some functions of the dynamical parameters and $\mathbf{k}$ (since they are rather cumbersome, we don't present them here). As we are interested in the difference of energy densities, we can neglect the first term in the brackets in

the equation above. Further, using Eq. (18), we can integrate over ω_E

$$\mathcal{E}_{\mathrm{L}} = \int\limits_0^{\Lambda} \int\limits_{-\Lambda - b_0}^{\Lambda - b_0} \frac{k dk\, dk_z}{(2\pi)^2} \frac{1}{\sqrt{W_1} + \sqrt{W_2}}\left[A_2(k_z) - \right.$$

$$\left. - W_1 - W_2 + \frac{A_1(k_z) - W_1 W_2}{\sqrt{W_1 W_2}} \right],$$

$$\mathcal{E}_{\mathrm{R}} = \int\limits_0^{\Lambda} \int\limits_{-\Lambda + b_0}^{\Lambda + b_0} \frac{k dk\, dk_z}{(2\pi)^2} \frac{1}{\sqrt{W_1} + \sqrt{W_2}}\left[A_2(-k_z) - \right.$$

$$\left. - W_1 - W_2 + \frac{A_1(-k_z) - W_1 W_2}{\sqrt{W_1 W_2}} \right], \tag{A10}$$

where $W_{1,2} = \left(\Delta^2 + v_{\mathrm{F}}^2(\mathbf{k}^2 + b^2) \right) \mp 2v_{\mathrm{F}} b\sqrt{\Delta^2 + k_z^2 v_{\mathrm{F}}^2}$.

1. X.-L. Qi and S.-C. Zhang, Rev. Mod. Phys. **83**, 831057 (2011).
2. M.Z. Hasan and C. L. Kaney Rev. Mod. Phys. **82**, 823045 (2010).
3. Y. Ando J. Phys. Soc. Jpn. **82**, 102001 (2013).
4. M.H. Cohen and E.I. Blount, Phil. Mag. **5**, 115 (1960).
5. P.A. Wolff, J. Phys. Chem. Solids **25**, 1057 (1964).
6. L.A. Fal'kovskii, Sov. Phys. Usp. **11**, 1 (1968).
7. V.S. Edel'man, Adv. Phys. **25**, 555 (1976); Sov. Phys. Usp. **20**, 819 (1977).
8. Z. Wang, Y. Sun, X. Chen, C. Franchini, G. Xu, H. Weng, X. Dai, and Z. Fang, Phys. Rev. B **85**, 195320 (2012).
9. Z. Wang, H. Weng, Q. Wu, X. Dai, and Z. Fang, Phys. Rev. B **88**, 125427 (2013).
10. Z.K. Liu, B. Zhou, Z.J. Wang, H.M. Weng, D. Prabhakaran, S.-K. Mo, Y. Zhang, Z.X. Shen, Z. Fang, X. Dai, Z. Hussain, and Y.L. Chen, Science **343**, 864 (2013).
11. M. Neupane, SuY. Xu, R. Sankar, N. Alidoust, G. Bian, C. Liu, I. Belopolski, T.-R. Chang, H.-T. Jeng, H. Lin, A. Bansil, F. Chou, and M.Z. Hasan, e-print arXiv:1309.7892v1 (2013).
12. S. Borisenko, Q. Gibson, D. Evtushinsky, V. Zabolotnyy, B. Buechner, and R. J. Cava, e-print arXiv:1309.7978v1 (2013).
13. H.-J. Kim, Ki-S. Kim, J.F. Wang, M. Sasaki, N. Satoh, A. Ohnishi, M. Kitaura, M. Yang, and L. Li, Phys. Rev. Lett. **111**, 246603 (2013).
14. E.V. Gorbar, V.A. Miransky, and I.A. Shovkovy, Phys. Rev. B **88**, 165105 (2013).
15. Z. Wang and S.-C. Zhang, Phys. Rev. B **87**, 161107(R) (2013).
16. H. Wei, S.-Po Chao, and V. Aji, Phys. Rev. Lett. **109**, 196403 (2012).
17. K.-Y. Yang, Y.-M. Lu, and Y. Ran, Phys. Rev. B **84**, 075129 (2011).
18. H.B. Nielsen and M. Ninomiya, Phys. Lett. B **130**, 389 (1983).

19. E.V. Gorbar, V.A. Miransky, and I.A. Shovkovy, Phys. Rev. C **80**, 032801(R) (2009).

20. E.V. Gorbar, V.A. Miransky, and I.A. Shovkovy, Phys. Rev. D **83**, 085003 (2011).

21. A.A. Zyuzin and A.A. Burkov, Phys. Rev. B **86**, 115133 (2012).

22. J.M. Cornwall, R. Jackiw, and E. Tomboulis, Phys. Rev. D **10**, 8, 2428 (1974).

23. A.I. Larkin and Y.N. Ovchinnikov, Sov. Phys. JETP **20**, 762 (1965).

24. P. Fulde and R.A. Ferrell, Phys. Rev. **135**, A550 (1964).

25. K. Malik, D. Das, D. Mondal, D. Chattopadhyay, A.K. Deb, S. Bandyopadhyay, A. Banerjee, J. of Applied Physics **112**, 083706 (2012).

26. J. Ziman, *Principles of the Theory of Solids* (Cambridge Univ. Press, Cambridge, 1972).

П.О. Сухачов

ГЕНЕРАЦІЯ ЩІЛИНИ
У ВЕЙЛІВСЬКИХ НАПІВМЕТАЛАХ З ЛОКАЛЬНОЮ
ЧОТИРЬОХФЕРМІОННОЮ ВЗАЄМОДІЄЮ

Р е з ю м е

Досліджено генерацію щілини у вейлівських напівметалах з локальною чотирьохферміонною взаємодією. Показано, що існує критичне значення константи зв'язку, яке відокремлює симетричну фазу та фазу з порушеною симетрією і описана відповідна фазова діаграма. Вивчено генерацію щілини в більш загальному класі вейлівських напівметалів з малою початковою щілиною та отримано квазічастинковий енергетичний спектр. Показано, що в цьому випадку динамічно згенерована щілина може привести до додаткового розщеплення квазічастинкових енергетичних зон.